Polymer Journal, Vol. 25, No. 10, pp 1087—1098 (1993)

Phase Behavior and Ordering Characteristics of Some Chain Molecules Dissolved in a Nematic Liquid Crystal, 4′-Methoxybenzylidene-4-*n*-butylaniline

Akihiro ABE, Emi IIZUMI, and Yuji SASANUMA

Department of Polymer Chemistry, Tokyo Institute of Technology, Ookayama, Meguro-ku, Tokyo 152, Japan

(Received March 26, 1993)

ABSTRACT: Phase diagrams were reported for binary mixtures comprising a series of dimethyl ethyleneglycol ethers $CH_3O(CH_2CH_2O)_xCH_3$ ($x=1$—3) (DMEG) and a nematogenic solvent 4′-methoxybenzylidene-4-*n*-butylaniline (MBBA) at low solute mole fraction. For a comparison purpose, measurements were also carried out for *n*-hexane hosted in the same solvent. Following Martire *et al.*, the slopes, β_N and β_I, of the nematic and isotropic phase boundary lines have been used as a measure of the compatibility of nonmesomorphic solutes with the nematic phase. The β values of the DMEG series were found to increase rapidly with the chain length in contrast to those reported for *n*-alkanes $CH_3(CH_2)_{n-2}CH_3$. The ^2H NMR technique was extensively employed to elucidate the orientational order of the individual components in the mixture. In accordance with the trend observed in the phase behavior, the DMEG series exhibit a greater reduction of nematic order when compared at the same solute concentration of hydrocarbon analogs. The deuterium quadrupolar splittings $\Delta\nu$ were observed for the methylene and methyl deuterons of the solute molecule. The ratio of quadrupolar splittings $\Delta\nu_i/\Delta\nu_j$ which represents the relative orientation of the CD bonds at sites i and j, were found to remain nearly invariant over a wide range of concentration and temperature. It has been concluded from the RIS analysis that the flexible chain molecules examined prefer to take somewhat more elongated forms to facilitate alignment in the nematic field as compared with those in the conventional isotropic solution.

KEY WORDS Ethyleneglycol Ethers / 4′-Methoxybenzylidene-4-*n*-butylaniline (MBBA) / *n*-Hexane / Phase Diagram / ^2H NMR / Nematic Conformation /

The thermodynamic stability of liquid-crystalline phase is largely determined by the steric repulsions and intermolecular attractions, both being anisotropic in reflection of asymmetry of molecular shapes. In a liquid-crystalline phase, the intermolecular interaction is cooperative, and molecular arrangements exhibit orientational correlations. Flexible chains, which tend to be a random-coil in the isotropic state, are soluble in liquid crystals only under some limited conditions. Phase diagrams have been reported for a number of binary systems comprising nematogenic compounds and chain molecules of various length.[1] Orendi and Ballauff[2] have studied mixtures of n-$C_{18}H_{38}$ or n-$C_{24}H_{50}$ with *p*-azoxyanisole (PAA) over a whole concentration range. The characteristic features of their phase diagrams can be summarized as follows. (1) In the dilute region, where *n*-alkane is regarded as the minor component, the nematic–isotropic equilibrium (N+I) can be observed. (2) At higher concentrations, two isotropic phases (I+I) coexists: the phase-boundary curve is characterized by an upper critical solution point. (3) Below a triphasic line, there is a wide two phase region (N+I). Oweimreen and Martire[3] extensively investigated the thermodynamic aspects involved in the NI equilibrium in region (1). In their

work, the slopes of the nematic and isotropic phase boundary lines have provided a measure of the nematic phase stability. *n*-Alkane molecules (n-C_8H_{18} to n-$C_{14}H_{30}$) were found to be more compatible with, thus less destructive to the ordered nematic phase of 4′-methoxybenzylidene-4-*n*-butylaniline (MBBA) as compared with some spherical or branched solutes having similar hard core volumes. An essentially identical behavior was observed in 4′-*n*-pentyl-4-cyanobiphenyl (5CB). Kronberg *et al.*[4] studied the molecular ordering of nematic MBBA, MBBA + 5 mol% of alkanes such as *n*-hexane, *n*-hexadecane, and their branched isomers by using a broad line NMR. From the observed dipolar splittings due to the ortho protons of the benzene ring, the orientational order of the MBBA molecule was estimated. While n-C_6H_{14} and n-$C_{16}H_{34}$ gave nearly superimposable order parameter *vs.* temperature curves, branched $C_{16}H_{34}$ was clearly more destructive, with lower order parameters, than n-$C_{16}H_{34}$. Martire[1] suggested in his review that the aligned environment should somewhat restrict the conformational freedom of *n*-alkane chains.

n-Alkanes are one of the simplest examples of chain molecules. In the free state, the *trans* form is more stable by about 0.5 kcal mol^{-1} relative to the alternative *gauche* form around the skeletal C–C bond.[5] The most preferred, lowest-energy conformation of the molecule is the planar *all-trans* arrangement.[6] When involved in the nematic phase, *n*-alkane chains may adopt relatively extended conformations in harmony with the environment. A small loss of entropy arising from such conformational restrictions may be compensated by the intermolecular interactions with the surroundings.

In the present work, we have extended similar thermodynamic studies for a series of dimethyl ethyleneglycol ethers, $CH_3O(CH_2CH_2O)_xCH_3$ ($x=1$—3). The characteristic feature of these chains is the decisive preference of *gauche* states around the OC–CO bond at variance with *n*-alkane chains. A detailed conformational analysis has been carried out for 1,2-dimethoxyethane (DME) and poly(oxyethylene) (POE) in various conventional solvents on the basis of NMR vicinal coupling constant measurements.[7] The energy difference (ΔE) between the *gauche* (*g*) and *trans* (*t*) state varies from -0.5 to -1.1 kcal mol^{-1} with the polarity of the medium. The values were found to be nearly identical between DME and POE in a given solvent. Our recent investigation revealed that DME prefers to take a *gauche* form even in the gas phase ($\Delta E = -0.4$ kcal mol^{-1}).[8] In the crystalline phase, the most stable form is known to be *tgt* for the moiety CO–C–C–OC for both compounds.[9] Our interests are to investigate phase behavior and ordering characteristics of the ethyleneglycol (EG) unit involved in a nematic solvent.

We have first studied phase behaviors of the system involving DME, the dimer ($x=2$) (abbreviated DMEG-2), or the trimer ($x=3$) (DMEG-3) in the nematic MBBA. The ^2H NMR technique was extensively employed to elucidate the orientational order of the individual components in the mixture. The conformational analysis of chain molecules was attempted according to a procedure similar to those previously adopted in the study of main chain dimer and polymer liquid crystals.[10,11] For a comparison purpose, measurements were also carried out for *n*-hexane hosted in MBBA. The number of quadrupolar splittings observed in the ^2H NMR measurements is two for DME, which is less than that (three) of *n*-hexane. The amount of information obtained through these measurements is not enough to elucidate an unequivocal solution.[11] The experimental data presented in this paper may also be interpreted in terms of several different models. To be more definite, proton–proton and carbon–carbon dipolar coupling analyses have been attempted by using isotope-labeled DME in an independent project. This will be the subject of the forthcoming paper.[12]

EXPERIMENTAL

Chemicals

Reagent grade samples of MBBA, DME, dimethyl diethyleneglycol ether (DMEG-2), and dimethyl triethyleneglycol ether (DMEG-3) are commercially available. *n*-Hexane-d_{14} ($CD_3(CD_2)_4CD_3$) was purchased commercially, and used without further purification. Partially deuterated compound were prepared as described below:

Dimethoxyethane-d_{10} (DMEG-d_{10}) CD_3O-$CD_2CD_2OCD_3$. Ethyleneglycol-d_4 is commercially available. The elimination reaction with methyliodide-d_3 was carried out according to the procedure described by Capinjola.[13] The fraction distilled at 80—88°C was collected.

Dimethyl diethyleneglycol ether-d_{14} (DMEG-2-d_{14}) $CD_3(CD_2CD_2O)_2CD_3$ *and Dimethyl triethyleneglycol ether-d_{18} (DMEG-3-d_{18})* CD_3-$(CD_2CD_2O)_3CD_3$. A mixture of diethyleneglycol-d_{10} and triethyleneglycol-d_{14} was first obtained by the reaction of ethyleneglycol-d_4 with ethyleneoxide according to the prescription described by Ishiguro *et al.*[14] After the elimination reaction with methyliodide-d_3,[13] DMEG-2 (bp 64.5°C/18—19 mmHg) and DMEG-3 (bp 64—65°C/1.5—2 mmHg) were respectively collected by a fractional distillation.

DMEG-2-d_4 ($CH_3OCD_2CH_2OCH_2CD_2O$-CH_3) and DMEG-3-d_4 ($CH_3OCD_2CH_2O$-$(CH_2)_2OCH_2CD_2OCH_3$). Diethyleneglycol-d_4 was obtained by reduction of diglycolic acid with lithium aluminum tetradeuteride. DMEG-2-d_4 was then derived through the reaction with methyliodide. 1,2-Bis(carboxymethyl)-ethane, a precursor of triethyleneglycol was prepared by following the procedure given by Abe *et al.*[15] Reduction with lithium aluminum tetradeuteride followed by methoxylation yielded DMEG-3-d_4.

4′-Methoxybenzylidene-4-n-butylaniline-2,6-d_2 (MBBA-d_2) CH_3O-C_6H_4-CHN-$C_6D_2H_2$-n-C_4H_9. 4′-*n*-Butylaniline-2,6-d_2 was prepared according to the prescription described by Zimmermann.[16] Condensation with 4-anisaldehyde was carried out by following Jones *et al.*[17] The reaction mixture was distilled under vacuum and the product was collected at 162—165°C/1 mmHg.

Measurements

Phase diagrams. To ensure a homogeneous mixing, solutions of given concentrations were prepared in the isotropic phase. Sample solutions (0.5 ml) were kept in sealed glass tubes with a diameter of 5mm, the atmosphere being replaced by a dry nitrogen. The sample containers were immersed in a thermostated water bath (Haak D3-G). The temperature was controlled with a precision ± 0.02°C. The onset of the biphasic region and its disappearance were determined visually on a cooling and heating cycle. The phase separation was clearly observed with a sharp boundary between the clear isotropic (at the top) and the turbid nematic phase (at the bottom).

Deuterium NMR. The ^{2}H NMR spectra of liquid-crystalline solutions were recorded at 76.65 MHz on JEOL JNM-GX-500 spectrometer equipped with variable-temperature controllers. Prior to the measurements, liquid-crystalline solutions were equilibrated in the spectrometer until homogeneous alignment was achieved. Measurements were carried out under a complete proton decoupling and nonspinning mode.

RESULTS

Phase Diagram

Shown in Figure 1 is the phase diagram derived for binary mixtures DME/MBBA (■, □) and *n*-hexane/MBBA (▲, △) at low mole fraction (x) of the solute, where $T^* = T/T_{NI}$, T_{NI} being the nematic-to-isotropic transition temperature of the pure liquid-crystalline solvent. Following Martire *et al.*,[1,3] the slopes of the phase boundary lines

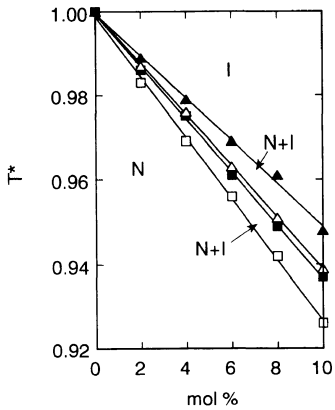

Figure 1. Phase diagram at low solute mole fraction. Reduced temperature T^* *vs.* mole fraction of DME (■, □) and *n*-hexane (▲, △) in MBBA.

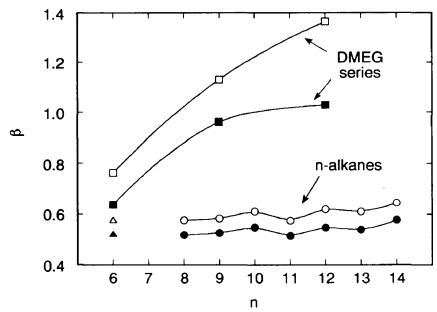

Figure 2. Slope of phase boundary lines as a function of skeletal-atom number (n) of solute chains. Lower line β_N is denoted by open symbols and upper line β_I by filled symbols. The slopes obtained for *n*-hexane are illustrated by triangles. The results for a series of *n*-alkanes ($n=8$—14) are taken from Oweimreen *et al.*'s works.

$$\beta_N = -\left(\frac{\partial T_N^*}{\partial x_N}\right) \quad (1)$$

$$\beta_I = -\left(\frac{\partial T_I^*}{\partial x_I}\right) \quad (2)$$

may be used as a measure of the compatibility of nonmesomorphic solutes with the nematic phase. Here, the notations x_N and x_I denote respectively the solute mole fractions in the coexisting phases at reduced temperatures T_N^* and T_I^*. The slopes obtained for DME/MBBA ($\beta_N = 0.763$ and $\beta_I = 0.636$) exceed the corresponding values ($\beta_N = 0.578$ and $\beta_I = 0.522$) for *n*-hexane/MBBA, suggesting that DME is more destructive than *n*-hexane in the nematic MBBA. In fact, the slopes observed for DME are nearly equivalent to those reported for highly branched solutes such as tetraethylethane $C(Et)_4$. According to Martire *et al.*,[1] the following relation should hold at an infinite dilution, where Henry's law becomes valid:

$$\frac{\Delta S_{NI}}{R} = \beta_I^{-1} - \beta_N^{-1} \quad (3)$$

Here R is the gas constant and ΔS_{NI} is the nematic–isotropic transition entropy of neat MBBA. The value of $\Delta S_{NI}/R$ determined by the direct calorimetry on a neat MBBA is 0.16.[1] The magnitudes of the $\beta_I^{-1} - \beta_N^{-1}$ term estimated from Figure 1 are 0.262 and 0.186, respectively, for DME/MBBA and *n*-hexane/MBBA. These results also suggest that DME is more perturbing in a nematic array than the hydrocarbon analog, *n*-hexane.

Phase behaviors of mixtures such as DMEG-2/MBBA and DMEG-3/MBBA have been examined in a similar manner. The slopes of the phase boundary lines β_N and β_I determined from the diagram are plotted against the number n of skeletal atoms of the solute in Figure 2. Also included for comparison are the β_N, β_I *vs.* n plot for the *n*-alkane/MBBA mixture reported by Oweimreen *et al.*[3] While the β values of the EG series, $CH_3(OCH_2CH_2)_xOCH_3$, tends to increase rapidly with the chain length, those for the *n*-alkane series, $CH_3(CH_2)_{n-2}CH_3$, remain essentially on the same level with a small odd–even oscillation.

The members of the EG series DME, DMEG-2, and DMEG-3 are respectively ether-analogs of *n*-hexane, *n*-nonane, and *n*-dodecane. In consideration of the enthalpy of mixing data reported for mixtures of small molecules,[18] aromatic compounds are usually more compatible with aliphatic ethers than with the corresponding hydrocarbons. The compounds in the EG series are more polar, and thus the solute-solvent interactions are

slightly more attractive in MBBA. The divergence in the phase behavior should be traced back to the conformational characteristics of these chains.

Deuterium NMR Measurements

Typical examples of the ^{2}H NMR spectra obtained for a mixture (0.5 mol%) of DME-d_{10}, DMEG-2-d_{14}, and DMEG-3-d_{18} with MBBA are shown in Figure 3. In these measurements, the solute and solvent molecules were labeled separately. In Figure 3a, the assignment to the methylene and methyl deuterons were facilitated by the characteristic profiles of the peaks.[19] The splittings due to the terminal methyl deuterons were also readily deduced from their characteristic profiles in Figures 3b (DMEG-2) and 3c (DMEG-3). The peaks arising from the $-CD_2CD_2-$ group situated in the central portion of DMEG-3 were easily detected in consideration of the intensity ratio. The resonance peaks of the two non-equivalent methylene groups in DMEG-2 and 3 were identified by employing partially deuterated samples such as DMEG-2-d_4 and DMEG-3-d_4. The splittings $\Delta\nu$ thus elucidated are illustrated in the figure. Shown in Figure 4

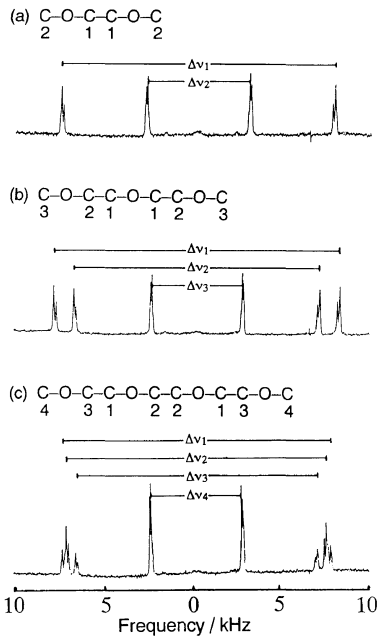

Figure 3. ^{2}H NMR spectra of (a) DME-d_{10}, (b) DMEG-2-d_{14}, and (c) DMEG-3-d_{18}, all dissolved in the nematic MBBA (0.5 mol%, 27.5°C). Assignments of the splittings are indicated by the position of skeletal carbon atoms in each diagram.

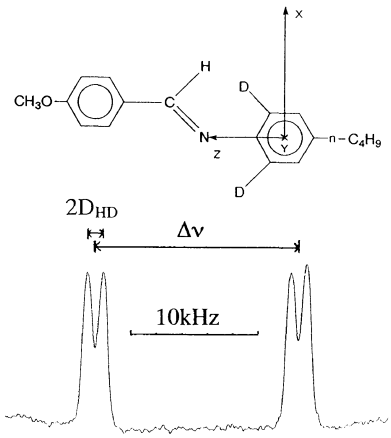

Figure 4. ^{2}H NMR spectrum of MBBA-d_2, containing 0.5 mol% of DME (27.5°C). Shown on the top of diagram is the definition of the molecular coordinate system, with which the orientational order parameters are deduced.

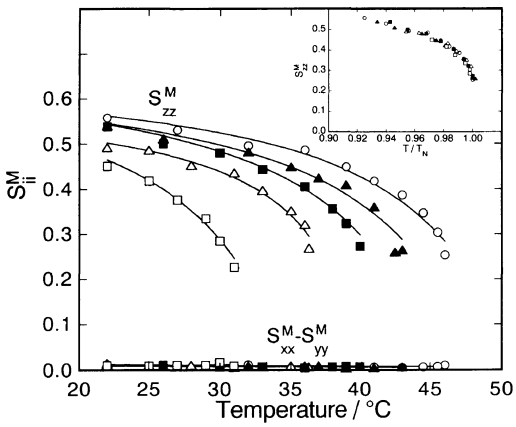

Figure 5. The Order parameter of MBBA (S^M_{ZZ}) as a function of temperature. The symbols denote ○ neat MBBA, and MBBA mixed with the following solutes: ■, DME (2.0 mol%); □, DME (6.0 mol%); ▲, *n*-hexane (2.0 mol%); △, *n*-hexane (6.0 mol%). Shown in the inset is the universal curve obtained by plotting S^M_{ZZ} against the temperature ratio T/T_N. The S^M_{ZZ} *vs.* T/T_N plots for DMEG-2/MBBA and DMEG-3/MBBA also fall on the curve but are omitted for clarity.

is the ^{2}H NMR spectrum obtained for MBBA-d_2, in which 2,6-positions of the aniline residue are specifically deuterated. The dipolar splittings D_{HD} due to the neighboring aromatic protons provide an additional information. The order parameters of MBBA have been elucidated from the observed $\Delta\nu$ and D_{HD} values according to the conventional procedure.[20] The definition of the molecular coordinate system is illustrated on the top of the diagram. In the following, the order parameters of the solvent, MBBA, will be differentiated from those of the solute molecule by a superscript M. The ^{2}H NMR measurements were carried out for mixtures of various compositions at different temperatures. For comparison, similar studies were performed for mixtures of n-hexane and MBBA. The peak assignment for n-hexane-d_{14} has been reported in literature.[26]

Figure 5 depicts the order parameters of MBBA, S_{ZZ}^M, as a function of temperature for the neat liquid crystal and for binary mixtures, DME/MBBA and n-hexane/MBBA, at different concentrations. The biaxiality of the MBBA molecule is very low in both systems. In accordance with the trend observed in the phase behavior, DME causes greater reduction of nematic order when compared at given solute concentrations. As suggested by Chen and Luckhurst,[21] and by Kronberg *et al.*,[4] a universal curve was obtained when the

Table I. ^{2}H NMR data for DME, n-hexane, DMEG-2, and DMEG-3, all observed in the nematic solvent MBBA

Concn	Temp.	$\Delta\nu_1$	$\Delta\nu_2$	$\Delta\nu_3$	$\Delta\nu_4$	D_1	D_2	D_3	D_4
mol%	°C	Hz	Hz	Hz	Hz	Hz	Hz	Hz	Hz
DME									
0.5	37.0	12876	4827			27.8	15.8		
	27.5	15264	5832			32.0	18.8		
	22.0	16400	6340			35.3	20.8		
2.0	27.5	14531	5551			30.8	18.0		
4.0	27.5	13206	5039			28.3	16.0		
6.0	27.5	11764	4485			24.0	13.8		
n-Hexane									
0.5	37.5	20413	18117	5874		45.3	39.0		
	27.5	24568	21842	7114		55.0	50.8		
	22.0	26398	23489	7676		60.5	54.3		
2.0	27.5	23818	21170	6885		53.8	49.5		
4.0	27.5	22394	19904	6470		50.8	46.5		
6.0	27.5	20938	18607	6050		46.3	42.3		
DMEG-2									
0.5	37.0	13354	11515	4246		25.8	23.8	14.3	
	27.5	15919	13679	5129		34.0	28.3	17.0	
	22.0	17083	14652	5548		36.8	30.0	18.8	
1.0	27.5	15430	13278	4970		32.3	25.8	16.0	
2.0	27.5	14334	12343	4621		31.5	25.0	15.3	
3.0	27.5	13181	11357	4253		28.5	22.5	13.8	
DMEG-3									
0.5	37.0	12428	12104	11178	4200	26.0	25.5	25.0	14.0
	27.5	14961	14505	13479	5154	30.8	30.0	28.8	17.3
	22.0	15510	15454	14218	5478	32.0	32.0	28.5	18.3
1.0	27.5	14186	13750	12801	4485	29.8	28.5	26.8	16.5
2.0	27.5	12653	12247	12343	4356	27.3	25.3	25.0	14.5
3.0	27.5	11382	11008	10289	3919	22.0	20.8	19.0	12.8

observed values of S_{ZZ}^{M} were plotted against the reduced temperature T/T_N (see the inset). The order parameters S_{ZZ}^{M} determined in this work are substantially smaller than those previously reported by Kronberg *et al.*[4] over the whole temperature range. The characteristic values of S_{ZZ}^{M} defined at the nematic-isotropic transition point ($T/T_N = 1.0$) were therefore found to be around 0.27—0.28 in comparison with those (*ca.* 0.36) of Kronberg *et al.* Studies were extended to include binary mixtures such as DMEG-2/MBBA and DMEG-3/MBBA. The ordered structure of the nematic solvent was found to be more efficiently affected by the presence of longer EG chains when compared at given mole fractions. These observations are at variance with those for a series of *n*-alkane/MBBA mixtures. The order parameters S_{ZZ}^{M} obtained above were also found to fall on a universal function of reduced temperature.

The deuterium quadrupolar splittings $\Delta\nu_i$ obtained for DME, DMEG-2, DMEG-3, and *n*-hexane confined in the nematic MBBA are summarized in Table I, where the dipolar couplings due to geminal deuterons observed concomitantly are also included. With the aid of other evidences, the signs of $\Delta\nu_i$'s thus obtained prove to be negative. For simplicity, absolute values are listed in the table. The results indicate that solute molecules tend to be more anisotropic as the nematic order of the surrounding solvent molecule increases either by decreasing the solute concentration or by lowering temperature. Since chain molecules are flexible, the observed splittings represent averages over all allowed conformations. As indicated in Figure 5, the ordering of MBBA molecules are largely dominated by the S_{ZZ}^{M} term, contribution from the biaxiality term being considerably small. We may assume similar characteristics for the orientation of solute molecules; *i.e.*, a proper molecular axis may be defined for each given conformer of the solute molecule. Within the validity of the single-ordering-matrix approximation, the ratio of quadrupolar splittings $\Delta\nu_i/\Delta\nu_j$, which represents the relative orientation of CD bonds at sites *i* and *j*, should be primarily sensitive to the conformation of the solute. The values of $\Delta\nu_i/\Delta\nu_1$, with $\Delta\nu_1$ indicating the largest splitting, are shown in Figure 6 as a function of temperature (a) and concentration (b). While the ratio $\Delta\nu_2/\Delta\nu_1$ of DME decreases slightly when plotted against temperature, it remains almost invariant with concentration. The values of $\Delta\nu_i/\Delta\nu_1$ ($i=2,3$) of *n*-hexane remain nearly constant over the entire temperature and concentration range studied. The experimental data given in Table I yielded similar plots for mixtures of DMEG-2/MBBA and DMEG-3/MBBA. With reasons stated above, these observations immediately suggest that the conformation of flexible solute should not be much affected by the orientational order of the nematic solvent.

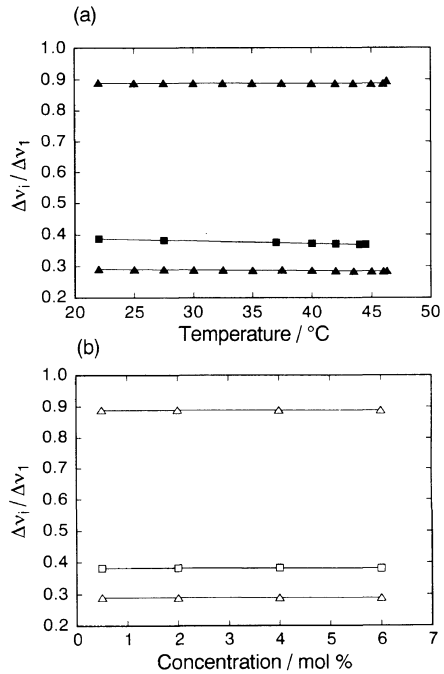

Figure 6. Variation of the deuterium quadrupolar splitting ratio $\Delta\nu_i/\Delta\nu_1$ as a function of temperature and concentration. (a): ■, DME; ▲, *n*-hexane, 0.5 mol% in MBBA. (b): □, DME; △, *n*-hexane, in MBBA at 27.5°C.

DISCUSSION

In order to describe an equilibrium between the nematic and isotropic phases as observed in this work, it is customary to adopt a model in which the intermolecular interaction consists of anisotropic repulsive and anisotropic attractive parts.[22,23] As demonstrated by Maier and Saupe,[24] contribution from the attractive part is most important in understanding the ordering behaviors of low-molecular-weight liquid crystals. In many examples, the temperature dependence of the order parameter has been satisfactorily described by the Maier–Saupe scheme in which the decrease in entropy owing to an anisotropic orientational distribution is compensated by the stabilization due to an anisotropic dispersion interaction

$$E = -\frac{1}{2}\left(\frac{A}{r^6}\right)S^2 \tag{4}$$

where A is called the anisotropy factor mainly determined by the anisotropy of the polarizability, r is the intermolecular distance, and S designates the orientational order parameter of mesogenic molecules. Since the transition under consideration is an order-disorder type, the role of the steric interaction must also be significant. The equation of state of nematics has been treated theoretically by several authors. Inclusion of steric contribution in thermodynamic expressions often leads to an appreciable overestimate of the order parameter at the transition.[23,25] Experimental observations described above indicate that flexible chains incorporated in liquid crystals take certain orientations by recognizing the uniaxial potential field of the environment. In Figure 7, the quadrupolar splittings $\Delta\nu_i$ observed for DME (a) and n-hexane (b) are plotted against the corresponding order parameters of the solvent MBBA. Since these two physical quantities, $\Delta\nu_i$ and S_{ZZ}^M, were determined by the independent measurements, experimental conditions are unnecessarily

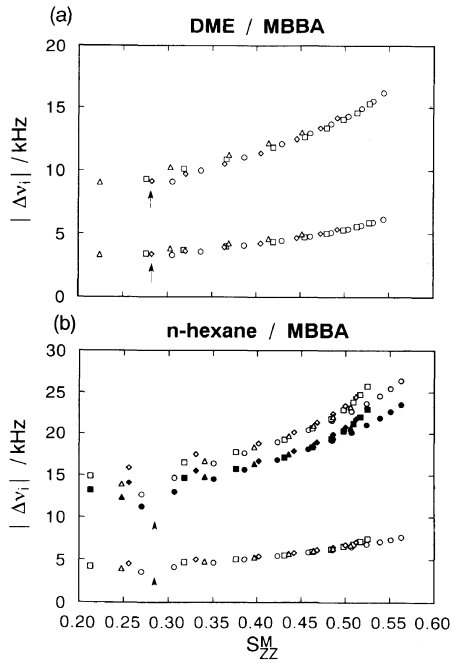

Figure 7. Plots of $\Delta\nu_i$ from the solute *vs.* S_{ZZ}^M of MBBA. (a) DME/MBBA: ○, 0.5; □, 2.0; ◇, 4.0; △, 6.0, units being mol%. (b) n-hexane/MBBA: ○●, 0.5; □■, 2.0; ◇◆, 4.0; △▲, 6.0, units being mol%. (Filled symbols are used to distinguish the data points for $i=2$ from $i=3$). The incipience of the biphasic region is indicated by the arrow.

corresponding with each other. For some data points, the S_{ZZ}^M values were taken from the smoothed curve (see Figure 5). Most of the experimental $\Delta\nu_i - S_{ZZ}^M$ pairs thus derived fall on a single curve within the experimental error. Similar universal plots have been obtained for DMEG-2 and DMEG-3 as well. It is interesting to note that the quadrupolar splittings of flexible components also reach a critical value in the region where the system becomes biphasic. These observations strongly suggest that flexible chains are also participating in the nematic interaction similar to those prescribed by eq 4 through the anisotropy of the polarizability.

As shown in Figure 6, the ratios $\Delta\nu_i/\Delta\nu_j$ which are only sensitive to the conformation of the flexible solute remain nearly invariant over a wide range of concentration and

temperature. With these results in mind, it may be interesting to compare the quadrupolar splitting ratios of *n*-hexane observed in various liquid-crystalline media. The ^{2}H NMR measurements reported by Samulski and his coworkers (0.5 mol% in Merck Phase V)[26] lead to $\Delta\nu_3/\Delta\nu_1=0.294$ and $\Delta\nu_2/\Delta\nu_1=0.888$, while the corresponding ratios obtained from Gochin *et al.*'s measurements (20 mol% in Kodak EK11650)[27] are 0.279 and 0.869 respectively. These values are comparable with those (0.288 and 0.888) found in the present work. The conformation of *n*-hexane molecule must be rather similar in all cases studied in spite of the fact that experimental conditions are quite divergent.

In our previous paper, we have analyzed the proton-proton dipolar coupling and deuterium quadrupolar splitting data reported respectively by Gochin *et al.*[27] and Janik *et al.*[26]

Table II. Summary of various RIS simulations for proton-proton dipolar couplings of *n*-hexane Experimental data taken from Gochin *et al.*'s work[a]

Proton pair	Experimental (COSY)	Calculated				
		This work			Gochin *et al.*[b]	Photinos *et al.*[c]
		A[d]	B	C		
1—2	1876 (±28)	1823	1750	1697	1792	1806
1—12	−206 (±13)	−171	−192	−208	−184	−191
1—4	−386 (±15)	−392	−354	−326	−366	−410
1—10	−322 (±14)	−277	−300	−318	−289	−288
1—6	−1034 (±25)	−961	−943	−930	−1025	−1016
1—8	−598 (±15)	−526	−594	−644	−591	−616
4—5	3974 (±34)	3895	3729	3607	3980	4053
4—10	−609 (±14)	−572	−721	−838	−543	−574
5—10	−713 (±18)	−852	−979	−1066	−789	−794
6—7	4487 (±34)	4366	4307	4262	4515	4483
6—8	43 (±12)	63	44	37	119	45
7—8	−190 (±12)	−193	−200	−211	−106	−189
4—6	186 (±14)	226	214	209	184	214
5—6	81 (±12)	70	59	46	28	79
4—8	−1616 (±25)	−1628	−1498	−1407	−1719	−1591
5—8	−1086 (±27)	−952	−1021	−1062	−1019	−1058
R/%		4.1	6.9	10.0	6.6	2.3
Conformer		Fraction (%)[e]				
ttt (1)		38.0	29.5	24.5	30.4	24.4
ttg (4)		7.2	7.4	7.3	8.3	8.7
tgt (2)		9.9	10.7	11.1	8.3	8.5
tgg (4)		1.9	2.7	3.3	2.3	2.8
g^+tg^+ (2)		1.3	1.8	2.2	2.3	2.8
g^+tg^- (2)		1.3	1.8	2.2	2.3	2.8
ggg (2)		0.4	0.7	1.0	0.6	0.9

[a] Reference 27.
[b] Reference 27 Model A.
[c] Reference 29.
[d] The simulation yielded $|\Delta\nu_3/\Delta\nu_1|=0.288$ and $|\Delta\nu_2/\Delta\nu_1|=0.876$. The order parameters of the molecular axis estimated concomitantly are $S_{ZZ}=0.196$ and $S_{XX}-S_{YY}=0.065$.
[e] In the isotropic state: *ttt* 18.8%, *ttg* 8.2%, *tgt* 8.2%, *ggg* 1.6%, estimated by using conformational energy parameters $E_\sigma=0.5$ and $E_\omega=3.0\,\mathrm{kcal\,mol^{-1}}$

according to our statistical model[11], in which the best-fit simulation was achieved through minimization of the error function (R) by the simplex method. The conformer fractions of n-hexane thus obtained were substantially different between the two sets of experimental data: *e.g.*, the fraction of the *all-trans* conformer was found to be 32.3 and 48.9%, respectively. These results are inconsistent with the aforementioned argument on the basis of the quadrupolar splitting ratios. Gochin *et al.*[27] have determined sixteen pairs of dipolar couplings in addition to three deuterium quadrupolar splittings. The latter results ($f_{ttt}=48.9\%$) derived from deuterium quadrupolar splitting data alone should be an overestimate of more elongated forms. We have tentatively repeated the simulation[28] by using our deuterium quadrupolar splitting ratios (see above) in combination with Gochin *et al.*'s proton-proton dipolar coupling (COSY) data.[27] In these calculations, high-energy forms such as $g^{\pm}g^{\mp}$ were excluded. Inclusion of such arrangements affected little the best-fit conformer set, but the R-value of the corresponding simulation was appreciably enhanced. The results are summarized in Table II, where calculations reported by Gochin *et al.*[27] and Photinos *et al.*[29] are also included for comparison. As indicated in the table, the observed proton–proton dipolar coupling data can be interpreted equally well by different statistical models, yielding somewhat divergent results. Our best-fit simulation yields a conformer set (A) which includes a relatively higher f_{ttt} value (38.0%) in comparison with those of the other groups: $f_{ttt}=30.4\%$ (Gochin *et al.*) and 24.4% (Photinos *et al.*). In the same table, the results of simulation obtained by adopting somewhat larger R values ($R=6.9$ and 10.0%) are also included to facilitate the comparison with those of the other groups. Sets B and C are qualitatively corresponding to Gochin *et al.*'s and Photinos *et al.*'s set, respectively. Although the best-fit results selected by minimizing the R-factor vary substantially depending on the characteristics of the theoretical model, the acceptable range of conformer fractions, which can be estimated around the best-fit set, may largely overlap each other. The conformer fractions calculated for the isotropic state are given in the footnote of the table. All these analyses definitely lead to a conclusion that n-hexane molecule favors somewhat extended forms when incorporated in the liquid-crystalline environment. The order parameters of the molecular axis have been calculated simultaneously. The values obtained for the best-fit set (A) are also listed in the footnote of the table.

The deuterium quadrupolar splitting data obtained for a series of dimethyl ethyleneglycol

Table III. Bond conformations of the DMEG series estimated by the RIS simulation of deuterium quadrupolar splitting ratios

	DME		DMEG-2		DMEG-3	
	In MBBA	Free state[a]	In MBBA	Free state[a]	In MBBA	Free state[a]
trans Fraction						
Bond 2 (C–O)	0.605—0.872	0.779	0.966—1.000	0.771	0.696—0.736	0.771
Bond 3 (C–C)	0.252—0.679	0.178	0.682—0.774	0.168	0.573—0.694	0.168
Bond 4 (C–O)			0.523—0.823	0.792	0.962—1.000	0.792
Bond 5 (C–O)					0.278—0.420	0.792
Bond 6 (C–C)					0.788—0.984	0.168
Axial ratio						
L/D	1.53—1.76	1.529	1.90—2.12	1.667	2.04—2.17	1.621

[a] Estimated by using conformational energy parameters $E_{\rho}=1.0$, $E_{\sigma}=-0.6$, $E_{\omega}=0.53\,\mathrm{kcal\,mol^{-1}}$.

ethers have been analyzed similarly. As manifestly shown in the aforementioned example, the experimental observations were found to be equally well reproduced by several sets of conformer fractions. In Table III, we report the range of bond conformations within which the iterative calculation converges with the R-factor less then 4%. For DME, the result of simulation was found to vary depending on the initial data set. The observed ratio $\Delta\nu_2/\Delta\nu_1=0.380$ can be satisfactorily reproduced over a broad range of conformer fractions: *e.g.*, several possible sets were found within ranges of $f_{tgt}=27$ to 37% and $f_{ttt}=6$ to 50%. In the isotropic state, the values of f_{tgt} and f_{ttt} are estimated to be 51.4% and 9.4%, respectively, on the basis of conformational energy parameters determined by the NMR vicinal coupling constant measurements in solution.[6] The conformational analysis of higher homologs DMEG-2 and DMEG-3 are also attempted in our single-ordering-matrix scheme. As indicated in Table III, the bond conformations estimated by simulations for $R<4\%$ cover a wide range. Also listed in the last row of the table are the length-to-breadth ratios (L/D) estimated for the nematic and isotropic forms, L and D of pseudo-cylinders being caluculated for each conformer by assuming van der Waals radii of the carbon, oxygen, and hydrogen atoms to be 1.70, 1.52, and 1.20 Å, respectively.[31] It is somewhat indecisive whether or not long-range conformational-correlations exist along the chain. Further elaborations are needed to deduce more reliable conformer fractions for DMEG-2 and DMEG-3 in MBBA. For DME, proton-proton and carbon-carbon dipolar coupling constants have been determined by using properly isotope-labeled samples. Combined use of these informations should lead to a more reliable estimate of conformer fractions adopted in liquid crystals. The results will be reported elsewhere.

Acknowledgment. The authors are grateful to the Asahi Glass Foundation for financial support of this work.

REFERENCES AND NOTES

1. G. R. Luckhurst and G. W. Gray, Ed.,"The Molecular Physics of Liquid Crystals," Academic Press, New York, N.Y., 1979.
2. H. Orendi and M. Ballauff, *Liq. Cryst.*, **6**, 497 (1989).
3. G. A. Oweimreen, G. C. Lin, and D. E. Martire, *J. Phys. Chem.*, **83**, 2111 (1979); G. A. Oweimreen and D. E. Martire, *J. Chem. Phys.*, **72**, 2500 (1980).
4. B. Kronberg, D. F. R. Gilson, and D. Patterson, *J. Chem. Soc., Faraday Trans. 2*, **72**, 1673, 1686 (1976).
5. A. Abe, R. L. Jernigan, and P. J. Flory, *J. Am. Chem. Soc.*, **88**, 631 (1966).
6. P. J. Flory, "Statistical Mechanics of Chain Molecules," Interscience, New York, N.Y., 1969.
7. K. Tasaki and A. Abe, *Polym. J.*, **17**, 641 (1985); A. Abe, K. Tasaki, and J. E. Mark, *Polym. J.*, **17**, 883 (1985); A. Abe, in "Comprehensive Polymer Science," Vol. 2, C. Booth and C. Price, Ed., Pergamon, Oxford, 1989, p 49.
8. K. Inomata and A. Abe, *J. Phys. Chem.*, **96**, 7934 (1992).
9. H. Matsuura, T. Miyazawa, and K. Machida, *Spectrochim. Acta A*, **29**, 771 (1973); H. Matsuura and H. Murata, *J. Raman Spectrosc.*, **12**, 144 (1982); H. Matsuura and H. Murata, *Chem. Lett.*, 169 (1978).
10. A. Abe and H. Furuya, *Mol. Cryst. Liq. Cryst.*, **159**, 99 (1988); A. Abe, H. Furuya, and D. Y. Yoon, *Mol. Cryst. Liq. Cryst.*, **159**, 151 (1988); A. Abe and H. Furuya, *Macromolecules*, **22**, 2982 (1989); A. Abe, *Makromol. Chem., Makromol. Symp.*, **53**, 13 (1992).
11. Y. Sasanuma and A. Abe, *Polym. J.*, **23**, 117 (1991).
12. E. Iizumi, Master's Dissertation, Tokyo Institute of Technology, 1993; A. Abe, N. Kimura, and E. Iizumi, to be published.
13. J. V. Capinjola, *J. Am. Chem. Soc.*, **67**, 1615 (1945).
14. T. Ishiguro, S. Kato, and Y. Akazawa, *Yakugaku Zasshi*, **63**, 282 (1943).
15. Y. Abe, C. Kato, D. Higo, T. Aoki, and H. Miyagawa, *Yukagaku*, **18**, 31 (1969).
16. H. Zimmermann, *Liq. Cryst.*, **4**, 591 (1989).
17. D. Jones, L. Creagh, and S. Lu, *Appl. Phys. Lett.*, **16**, 61 (1970).
18. J. S. Rowlinson and F. L. Swinton, "Liquids and Liquid Mixtures," 3rd ed., Butterworths, London, 1982.
19. S. Hsi, H. Zimmermann, and Z. Luz, *J. Chem. Phys.*, **69**, 4126 (1978).
20. J. W. Emsley, Ed., "Nuclear Magnetic Resonance of Liquid Crystals," D. Reidel Publishing Company, Dordrecht, 1983; J. W. Emsley, G. R. Luckhurst, and G. N. Shilstone, *Mol. Phys.*, **53**, 1023 (1984).
21. D. H. Chen and G. R. Luckhurst, *Trans. Faraday*

Soc., **65**, 656 (1969).
22. P. G. de Gennes, "The Physics of Liquid Crystals," Oxford University Press, Oxford, 1975.
23. G. Vertogen and W. H. de Jeu, "Thermotropic Liquid Crystals, Fundamentals," Springer-Verlag, Berlin, 1988.
24. W. Maier and A. Saupe, *Z. Naturforsch.*, **14a**, 882 (1959); *ibid.*, **15a**, 287 (1960).
25. P. J. Flory and G. Ronca, *Mol. Cryst. Liq. Cryst.*, **54**, 289, 311 (1979).
26. B. Janik, E. T. Samulski, and H. Toriumi, *J. Phys. Chem.*, **91**, 1842 (1987).
27. M. Gochin, A. Pines, M. E. Rosen, S. P. Rucker, and C. Schmidt, *Mol. Phys.*, **69**, 671 (1990); M. Gochin, Z. Zimmermann, and A. Pines, *Chem. Phys. Lett.*, **137**, 51 (1987).
28. Computational procedures and geometrical parameters required in the calculation have been given in ref. 11. In the present simulation, conformational energy parameters σ_2, σ_3, and order parameters S_{ZZ}, $S_{XX}-S_{YY}$ were adjusted so as to reproduce experimental observations, contribution from off-diagonal elements of the ordering matrix being ignored.
29. D. J. Photinos, B. Janik Poliks, E. T. Samulski, A. F. Terzis, and H. Toriumi, *Mol. Phys.*, **72**, 333 (1991); In a more recent work,[30] they have proposed a nine-state scheme instead of the conventional three-state model. For a purpose of comparison, we cite their results calculated by using the latter model.
30. D. J. Photinos, E. T. Samulski, and A. F. Terzis, *J. Phys. Chem.*, **96**, 6979 (1992).
31. A. Bondi, *J. Phys. Chem.*, **68**, 441 (1964).